



1           **Dissolved Inorganic Nutrients in the Western Mediterranean Sea (2004-2017)**

2           Malek Belgacem<sup>1,2</sup>, Jacopo Chiggiato<sup>1,\*</sup>, Mireno Borghini<sup>1</sup>, Bruno Pavoni<sup>2</sup>, Gabriella Cerrati<sup>3</sup>,  
3           Francesco Acri<sup>1</sup>, Stefano Cozzi<sup>4</sup>, Alberto Ribotti<sup>5</sup>, Marta Álvarez<sup>6</sup>, Siv K. Lauvset<sup>7,8</sup>, Katrin  
4           Schroeder<sup>1</sup>

5           <sup>1</sup> CNR-ISMAR, Arsenale Tesa 104, Castello 2737/F, 30122 Venezia, Italy

6           <sup>2</sup> Dipartimento di Scienze Ambientali Informatica e Statistica, Università Ca' Foscari Venezia,  
7           Campus Scientifico Mestre, Italy

8           <sup>3</sup> ENEA, Department of Sustainability, S. Teresa, Marine Environmental center, 19032 Pozzuolo di  
9           Lerici (SP), Italy

10          <sup>4</sup> CNR-ISMAR, Area Science Park – Basovizza, 34149 Trieste, Italy

11          <sup>5</sup> CNR-IAS, Loc. Sa Mardini snc, Torregrande, 9170 Oristano, Italy

12          <sup>6</sup> Instituto Español de Oceanografía, IEO, A Coruña, Spain

13          <sup>7</sup> NORCE Norwegian Research Centre, Bjerknes Centre for Climate Research, 5007 Bergen, Norway

14          <sup>8</sup> Geophysical Institute, University of Bergen and Bjerknes Centre for Climate Research, 5007  
15          Bergen, Norway

16          \*Corresponding author's email: [jacopo.chiggiato@ismar.cnr.it](mailto:jacopo.chiggiato@ismar.cnr.it)

17

18          **Abstract**

19          Long-term time-series are a fundamental prerequisite to understand and detect climate shifts and  
20          trends. Understanding the complex interplay of changing ocean variables and the biological  
21          implication for marine ecosystems requires extensive data collection for monitoring and hypothesis  
22          testing and validation of modelling products. In marginal seas, such as Mediterranean Sea, there are  
23          still monitoring gaps, both in time and in space. To contribute filling these gaps, an extensive dataset  
24          of dissolved inorganic nutrients profiles (nitrate, NO<sub>3</sub>; phosphate, PO<sub>4</sub><sup>3-</sup>; and silicate, SiO<sub>2</sub>) have been  
25          collected between 2004 and 2017 in the Western Mediterranean Sea and subjected to quality control  
26          techniques to provide to the scientific community a publicly available, long-term, quality controlled,



27 internally consistent biogeochemical data product. The database includes 870 stations of dissolved  
28 inorganic nutrients sampled during 24 cruises, including temperature and salinity. Details of the  
29 quality control (primary and secondary quality control) applied are reported. The data are available in  
30 PANGAEA (<https://doi.pangaea.de/10.1594/PANGAEA.904172>, Belgacem et al. 2019)

31 **Keywords:** Mediterranean Sea, Dissolved Inorganic Nutrient, biogeochemistry

32

### 33 1 Introduction

34 Dissolved inorganic nutrients are important tracers of biological cycles, new production, natural and  
35 anthropogenic sources and transport processes (Bethoux, 1989; Bethoux et al., 1992) They are non-  
36 conservative seawater constituents, whose distribution is controlled by both physical (such as  
37 convection, advection, mixing and diffusion) and biogeochemical (such as primary production and  
38 respiration) processes. Very schematically, nutrients are continuously removed from the sea surface  
39 (due to primary production) and regenerated in the mesopelagic layer (due to respiration). Moreover,  
40 the sinking of biogenic matter and its degradation increases the nutrient concentrations in the  
41 intermediate and deep-water masses over time. To identify the limiting factors for biological  
42 production in the oceans we need to understand the underlying chemical constraints and especially the  
43 macro- and micronutrients spatial and temporal variations. Dissolved inorganic nutrients may be used  
44 to trace water masses, to assess mixing processes, and to understand the biogeochemical conditions of  
45 their formation regions. Understanding the complex interplay of changing ocean variables and the  
46 biological implication for marine ecosystems is a difficult task and requires not only modelling, but  
47 also extensive data collection for monitoring and hypothesis testing and validation. The latter has been  
48 done in the open oceans (e.g. GLODAP), but for marginal seas such as the Arctic Ocean or the  
49 Mediterranean Sea there are still monitoring gaps, both in time and in space.



50 The Mediterranean Sea has been identified as a region significantly affected by ongoing climatic  
51 changes, like warming and decrease in precipitation (Giorgi, 2006). In addition, it is a region  
52 particularly valuable for climate change research because it behaves like a miniature ocean (Bethoux  
53 et al., 1999) with a well-defined overturning circulation characterized by spatial and temporal scales  
54 much shorter than for the global ocean, with a turnover of only several decades. The Mediterranean  
55 Sea is therefore a potential model to study global patterns that will be experienced in the next decades  
56 worldwide, not only regarding ocean circulation, but also the marine biota (Lejeusne et al., 2010).  
57 Several environmental variables can act as stressors for marine ecosystems (Boyd, 2011), by which  
58 climatically driven ecosystem disturbances are generated. These changes affect, among others, the  
59 distribution of biogeochemical elements (including nutrients) and the functioning of the biological  
60 pump.

61 The Mediterranean, compared to the world's oceans, is also more influenced by continental nutrient  
62 inputs (Dardanelles, river runoff, submarine groundwater discharge and atmospheric inputs): and since  
63 all these inputs go in the same direction of high nitrate to phosphate (N:P) ratios, the N:P ratios in the  
64 Mediterranean are anomalously high compared to the “classical” Redfield ratio, indicating a general P-  
65 limitation for this sea, which becomes stronger along a west-to-east gradient.

66 Within this context, the aim of this paper is to compile an extensive dataset of dissolved inorganic  
67 nutrients profiles (nitrate,  $\text{NO}_3^-$ ; phosphate,  $\text{PO}_4^{3-}$ ; and silicate,  $\text{SiO}_2$ ) collected between 2004 and 2017  
68 in the Western Mediterranean Sea (WMED), to describe the quality control techniques and to provide  
69 to the scientific community a publicly available, long-term, quality controlled, internally consistent  
70 biogeochemical data product, contributing to previously published Mediterranean datasets like the  
71 Medar/Medatlas dataset (Fichaut et al., 2003).

72 Both original and quality-controlled data are available in PANGAEA,

73 <https://doi.pangaea.de/10.1594/PANGAEA.904172>



74 Coverage: 44°N-35°S; -6°W-14°E  
75 Location Name: Western Mediterranean Sea  
76 Date start: May 2004  
77 Date end: November 2017

## 78 **2 Dissolved inorganic nutrient data collection**

### 79 **2.1. The CNR dissolved inorganic nutrient data in the WMED**

80 Long-term time-series, such as the OceanSites global time series ([www.oceansites.org](http://www.oceansites.org)), are a  
81 fundamental prerequisite to understand and detect climate shifts and trends. However, biogeochemical  
82 time-series are still restricted to the northern western Mediterranean Sea (three biogeochemical fixed  
83 platforms). Yet, inorganic nutrients in the Mediterranean Sea has received more attention in recent  
84 years, and various datasets have been compiled to understand its unique characteristics such as the  
85 PERSEUS (Policy-oriented marine environmental research in the southern European seas), a database  
86 that included 100 cruises collected within PERSEUS itself in addition to those from projects like  
87 Sesame, or data managing systems as SeaDataNet and EMODnet, or the MEDAR/MEDATLAS  
88 (1999-2004) database.

89 The dataset presented here consists of 24 oceanographic cruises (Fig. 1 and Table 1) conducted in the  
90 WMED on board of research vessels run by the Italian National Research Council (CNR) and the  
91 Science and Technology Organisation Centre for Maritime Research and Experimentation (NATO-  
92 STO CMRE). All cruises were merged into a unified dataset with 870 nutrient stations and ~ 9666  
93 data points over a period of 13 years (2004-2017). The overall spatial distribution of the stations  
94 covers the whole WMED, but the actual distribution strongly varies depending on the specific cruise  
95 (which can be seen on the right side of Fig. 9) and most of the data are collected along sections. At all  
96 stations, pressure, salinity, potential temperature were measured with a CTD-rosette system consisting  
97 of a CTD SBE 911 plus and a General Oceanics rosette with 24 12L Niskin Bottles. Temperature



98 measurements were performed with an SBE-3/F thermometer with a resolution of  $10^{-3}$  °C;  
99 conductivity measurements were performed with an SBE-4 sensor with a resolution of  $3 \cdot 10^{-4}$  S/m.  
100 The probes were calibrated before and after each cruise. During all CNR cruises, redundant sensors  
101 were often used for both temperature and salinity measurements.

102 Seawater samples for dissolved inorganic nutrient measurements were collected during the CTD up-  
103 cast at standard depths (with slight modifications according to the depth at which the deep chlorophyll  
104 maximum was detected). The standard depths are usually 5, 25, 50, 75, 100, 200, 300, 400, 500, 750,  
105 1000, 1250, 1500, 1750, 2000, 2250, 2500, 2750, 3000 m. No filtration was employed, but nutrient  
106 samples were immediately stored at  $-20$  °C.

## 107 **2.2. Reference inorganic nutrient data**

108 In addition to the data collected during the above-mentioned cruises, and in order to perform the  
109 secondary quality control (described below), we identified five reference cruises (Table 2), based on  
110 their spatial and temporal distribution of the data and the reliability of the measurements (see Fig. 2 –  
111 Table.1S Fig.1S). Cruises 06MT20110405 and 06MT20011018 are the only two Mediterranean  
112 cruises included in the publicly available Global Ocean Data Analysis Project version 2 (GLODAPv2,  
113 (Olsen et al., 2016)). These cruises, on board the R/V Meteor, provide a reliable reference because  
114 nutrient analysis strictly followed the recommendation of the World Ocean circulation experiment  
115 (WOCE) and the GO-SHIP protocols (Tanhua et al., 2013). Cruises 29AH20140426 and  
116 48UR20070528 are included in the CARIMED data product and have undergone rigorous quality  
117 control following GLODAP routines. Finally, 29AJ20160818 was carried out in the framework of the  
118 MedSHIP programme (Schroeder et al., 2015) and its data are available at  
119 <https://doi.org/10.1594/PANGAEA.902293> (Tanhua, 2019).

## 120 **3 Analytical methods for inorganic nutrients**



121 For all cruises, nutrient determination (nitrate, orthosilicate and orthophosphate) was carried out  
122 following standard colorimetric methods of seawater analysis, defined by Grasshoff et al. (1999) and  
123 (Hansen and Koroleff, 1999). For inorganic phosphate, the method is based on the reaction of the ions  
124 with an acidified molybdate reagent to yield a phosphomolybdate heteropoly acid, which is then  
125 reduced to a blue-colored compound (absorbance measured at 880 nm). Inorganic nitrate is reduced  
126 (with cadmium granules) to nitrite that react with an aromatic amine leading to the final formation of  
127 the azo dye (measured at 550 nm). Then, the nitrite separately determined must be subtracted from the  
128 total amount measured to have only the nitrate. The determination of dissolved silicon is based on the  
129 formation of a yellow silicomolybdic acid reduced with ascorbic acid to blue-colored complex  
130 (measured at 820 nm, see (Hansen and Koroleff, 1999)).

131 The analytical method was performed using four different models of autoanalyzer in three laboratories  
132 (ENEA analysed all cruises with the following exceptions: cruise #23 and cruise #24 were analysed by  
133 CNR-ISMAR. From 2004 to 2013 nutrients were analysed by a continuous-flow system multichannel  
134 (Auto Analyzer Bran+Luebbe III Generation) while for those of 2015 (cruise #23) an OI-Analytical  
135 (Flow Solution III) flow-segmented autoanalyzer was used, with a detection limit of 0.01 $\mu$ M for  
136 nitrate+nitrite, 0.01 $\mu$ M for phosphate and 0.05 for silicate. Nutrient concentrations for the 2017 cruise  
137 (cruise #24) were measured by the Systea discrete analyzer EasyChem Plus, considering a detection  
138 limit of 0.1 $\mu$ M for nitrate, 0.01 $\mu$ M for phosphate and 0.02 $\mu$ M for silicate.

139 Measures from the autoanalyzer were reported in  $\mu$ mol L<sup>-1</sup>. Since measures of salinity and temperature  
140 were also available, nutrient concentrations were converted to the standard unit  $\mu$ mol kg<sup>-1</sup>, according  
141 to the laboratory analytical temperature (20°C). Data from nutrient analysis were then merged to CTD  
142 bottle data. Note that sample storage and freezing duration varied greatly from one cruise to another  
143 (Table 3 shows the cruises where this exceeded 1 year).

#### 144 **4 Quality control methods**



145 Combining nutrient data from different sources, collected by different operators, stored for different  
146 amounts of time, and analysed by multiple laboratories, is not a straightforward task. This is widely  
147 recognized in the biogeochemical oceanographic community, and since the 1990s several studies and  
148 programmes (e.g. World Ocean Database, World Ocean Atlas, World Ocean Circulation Experiment)  
149 have been devoted to facilitate the exchange of oceanographic data and develop quality control  
150 procedures to compile databases by the estimation of systematic errors (Gouretski and Jancke, 2001)  
151 to increase the intercomparability, generate consistent data sets and accurately observe the long-term  
152 change.

153 An example of a first quality control procedure is the use of certified standardizations that are  
154 available for salinity (IAPSO salinity standard by OSIL) and temperature (SPRT, Standard Platinum  
155 Resistance Thermometer). As for the inorganic carbon, total alkalinity and inorganic nutrients  
156 (Aoyama et al., 2016; Dickson et al., 2003), certified reference materials (CRM) have been recently  
157 made available for oceanographic cruises. However, since CRM are not always available or used for  
158 biogeochemical oceanographic data, (Lauvset and Tanhua, 2015) developed a secondary quality  
159 control tool to identify biases in deep data and from that estimate accuracy. The method suggests  
160 adjustments that reduce cruise to cruise biases, increase accuracy and allow for the inter-comparison  
161 between data from various sources. This approach, based on a crossover and inversion method  
162 (Gouretski and Jancke, 2001; Johnson et al., 2001), was used to generate the CARbon IN Atlantic  
163 ocean (CARINA, see (Hoppema et al., 2009)), GLODAPv2 (Olsen et al., 2016) and PACIFICA  
164 (Suzuki et al., 2013) databases.

#### 165 **4.1 Primary Quality control**

166 Each individual cruise was first subjected to a primary quality control (QC) that included a check of  
167 apparent and extreme outliers in CTD salinity, nitrate, phosphate and silicate. Each parameter included  
168 a quality control flag, following standard WOCE flags (Table 3).



169 The surface (0-250 db) layer was difficult to flag since its overall coefficient of variation (CV, defined  
170 as standard deviation over mean) for nitrate (1.16), phosphate (1.005) and silicate (0.75) was high due  
171 to air-sea interaction and the complexity of biological processes (Muniz et al., 2001) occurring in this  
172 layer. These influences are of reduced importance in the intermediate (250-1000 db) layer (nitrate  
173 CV=0.23, phosphate CV=0.31, silicate CV=0.24) and the deep (>1000 db) layer (nitrate CV=0.15,  
174 phosphate CV=0.22, silicate CV=0.14). Flags in the upper layer were thus set based on atypical  
175 distribution of measurements within depth ranges defined according to standard depths (0-10, 10-30,  
176 30-60, 60-80, 80-160, 160-260, 260-360, 360-460, 460-560, 560-1000 m). Below 1000 db, however, a  
177 rigorous flagging was performed including a check of nitrate to phosphate (N:P) and nitrate to silicate  
178 (N:Si) ratios, since the secondary QC (described in section 4.2) only evaluates measurements with  
179 WOCE flag 2. We considered as outlier any value that departs from the median by more than three  
180 median absolute deviations.

181 An overview of the nutrient distribution is provided with scatter plots, showing also the flagged  
182 measurements (Fig. 3). Each measurement was flagged 2 (“good”) or flagged 3 (“questionable”): 4.1%  
183 of nitrate data, 3.37% of phosphate data, 3.16% of silicate data, and 0.07% of CTD salinity data were  
184 considered outliers and flagged 3. As highlighted by (Tanhua et al., 2010), the primary QC can be  
185 subjective depending on the expertise of the person flagging the data, thus flagging could bring in  
186 some uncertainties.

187 In order to have a first assessment of the precision of each cruise measurements, the standard deviation  
188 of data deeper than 1000 db was calculated (Table 4). Overall, the standard deviation in the deep layer  
189 varied between 0.51 and 1.41  $\mu\text{mol kg}^{-1}$  for nitrate, between 0.1 and 1.64  $\mu\text{mol kg}^{-1}$  for silicate and  
190 between 0.025 and 0.078  $\mu\text{mol kg}^{-1}$  for phosphate. Cruises #3, #6 and #9 had the largest spatial  
191 extension (visible on the right side of Fig. 9) with an important number of samples over the entire area  
192 and the geographical variability of the distribution in dissolved inorganic nutrients results thus in the  
193 largest standard deviations. Conversely, cruises with smaller spatial coverages have lower standard





194 deviations. Therefore, a relatively small spatial coverage and high standard deviation is considered as  
195 indicative of data with low precision (Olsen et al., 2016). This applies to cruises #1, #5, and #16.  
196 Samples of nitrate and phosphate of cruise #5 have a standard deviation of  $1.35 \mu\text{mol kg}^{-1}$  and  $0.07$   
197  $\mu\text{mol kg}^{-1}$ , respectively, despite the small spatial coverage (right side of Fig.9). Cruise #1, with few  
198 stations in the Tyrrhenian Sea and 21 samples below 1000 db, has standard deviations of  $1.25 \mu\text{mol kg}^{-1}$   
199  $^1$  for nitrate,  $0.06 \mu\text{mol kg}^{-1}$  for phosphate and  $1.64 \mu\text{mol kg}^{-1}$  for silicate. A comparison with the  
200 deviations from e.g. cruise # 2, carried out in the same year and e.g. cruise #17 (with a similar cruise  
201 track), confirms the lower precision of the data of #1. Similar considerations apply to the quality of  
202 nitrate samples from cruise #16, covering a small area in the Sicily Channel, compared to cruise #14  
203 carried out in the same year but with a larger spatial coverage (right side of Fig. 9). Deep silicate  
204 measurements of cruise #6 have twice the standard deviation of silicate data of cruise #8 from the  
205 same year. This is again suggestive of limited precision. On the other hand, trying to explain the  
206 source of relatively high standard deviations in specific cruises is not always straightforward

207

208

#### 209 **4.2 Secondary Quality control: the crossover analysis**

210 The method used to perform the secondary QC on the dissolved inorganic nutrient dataset in the  
211 WMED makes use of the quality-controlled reference data described in section 2.2, and the crossover  
212 analysis toolbox developed by (Tanhua, 2010) and (Lauvset and Tanhua, 2015). The computational  
213 approach is based on comparing the cruise data set to a high-quality reference data set to quantify  
214 biases, described in detail by (Tanhua et al., 2010). Here, we summarize the technique with emphasis  
215 on inorganic nutrient.

216 The first step consisted of selecting reference data, as described in section 2.2. The second step is the  
217 crossover analysis that was carried out using a MATLAB Toolbox (available online:



218 [https://www.nodc.noaa.gov/ocads/oceans/2nd\\_QC\\_Tool/](https://www.nodc.noaa.gov/ocads/oceans/2nd_QC_Tool/)) where crossovers are generated as  
219 difference between two cruises using the “running cluster” crossover routine. Each cruise is thus  
220 compared to the chosen set of reference cruises. For each crossover, samples deeper than 1000 db are  
221 selected within a predefined maximum distance set to 2°arc distance, defined as a crossing region, to  
222 ensure the quality of the offset with a minimum number of crossovers and to minimize the effect of the  
223 spatial change. The reason to select measurements deeper than 1000 db, is to remove the high  
224 frequency variability associated to mesoscale features, biological activity and the atmospheric forcing  
225 acting in the upper layers, that might induce changes in biogeochemical properties of water masses.  
226 On the other hand, also the deep Mediterranean cannot be considered truly “unaffected”, as it is  
227 intermittently subjected to ventilation (Schroeder et al., 2016; Testor et al., 2018) and the real  
228 variability can be altered in adjusting data. The computational approach takes this into account, since  
229 weights are given to the less variant profile in the crossing region within each cruise so that the natural  
230 variation is not altered (for further details see (Lauvset and Tanhua, 2015)).

231 Before identifying crossovers, each profile was interpolated using the piecewise cubic Hermite method  
232 and the distance criteria outlined in (Lauvset and Tanhua, 2015), their Table 1, and detailed in (Key et  
233 al., 2004). The crossover is a comparison between each interpolated profile of the cruise being  
234 evaluated and the interpolated profile of the reference cruise. The result is a weighted offset (defined  
235 as difference cruise/reference) and a standard deviation of the offset. The standard deviation is  
236 indicative of the precision; however, it is important to note that this assumption only works because it  
237 is a comparison to a reference, and the absolute offset is indicative of accuracy.

238 The third step consists in evaluating and selecting the suggested correction factor, that was calculated  
239 from the weighted mean offset of all crossovers found between the cruise and the reference data set,  
240 involving a somehow subjective process.

241 For inorganic nutrients, offsets are multiplicative so that a weighted mean offset > 1 means that the  
242 measurements of the corresponding cruise are higher than the measurements of the reference cruise in



243 the crossing region and applying the adjustment would decrease the measured values. The magnitude  
244 of an increase or a decrease is the difference of the weighted offset from 1. In general, no adjustment  
245 smaller than 2% (accuracy limit for nutrient measurements) is applied (detailed description is found in  
246 (Hoppema et al., 2009; Lauvset and Tanhua, 2015; Olsen et al., 2016; Sabine et al., 2010; Tanhua et  
247 al., 2010)).

248 The last step is the computation of the weighted mean (WM) to determine the internal consistency and  
249 quantify the overall accuracy of the adjusted inorganic nutrient dataset, referring to what has been  
250 described by (Hoppema et al., 2009; Sabine et al., 2010; Tanhua et al., 2009), with the difference that  
251 our assessment is based on the offsets with respect to a set of reference cruises. The accuracy was  
252 computed from the individual weighted offsets. The weighted mean, which will be discussed in  
253 section 5.4., was computed using the individual weighted offset (D) of number of crossovers (L) and  
254 the standard deviation ( $\sigma$ ):  $WM = \frac{\sum_{i=1}^L D(i)/(\sigma(i))^2}{\sum_{i=1}^L 1/(\sigma(i))^2}$

## 255 5 Results of the secondary QC and recommendations

256 The secondary QC revealed various multiplicative corrections necessary for nitrate, phosphate and  
257 silicate. Four cruises (#7, #11, #19, and #21) were not considered in the crossover analysis: cruises #7  
258 and #11 do not have enough (at least 3 to get valid statistics) stations > 1000 db, while cruises #19 and  
259 #21 were outside the spatial coverage of the reference cruises. Cruises that were not used for the  
260 crossover analysis are not included in the adjusted dataset.

261 Overall, we found a total number of 73 individual crossovers for nitrate, 72 for phosphate and 54 for  
262 silicate. An example of the running cluster crossover output is displayed in Fig.4. Results of the  
263 crossover analysis is an adjustment factor by cruise that are shown in Tables 5 and Fig. 5-6-7 that was  
264 calculated from the weighted mean of absolute offset summarized in Table 6 and Fig. 2S-3S-4S. Table  
265 6 details the improvement of the weighted mean of absolute offset by cruise prior and after



266 adjustments, the information is also displayed graphically in Fig. 2S-3S-4S. Cruises are in  
267 chronological order in all figures and tables.

## 268 **5.1 Nitrate**

269 The crossover analysis suggests adjustments for nitrate concentrations on 15 cruises, from 0.94 to 0.98  
270 (<1) and from 1.02 to 1.34 (>1) (Table 5 and Fig.5). Offsets suggest that deep measurements of cruises  
271 #1, #3, #4, #5, #6, #8, #12, #13, #15, #16, #23 and #24 need to be adjusted towards higher  
272 concentrations, when compared to the respective reference (Fig.2S). Nitrate data from cruises #2, #9  
273 and #10 on the other hand were higher than the reference cruises and require a downward adjustment.  
274 Finally, five cruises (#14, #17, #18, #20, and #22) were consistent with the reference data and no  
275 adjustment was necessary. Considering the weighted mean of absolute offset after adjustments shown  
276 in Table 6, two cruises require large correction factors and are still outside the accuracy threshold:  
277 cruises #5 and #24 (Fig. 5). These cruises are considered in detail later (section 5.4).

278

## 279 **5.2 Phosphate**

280 For phosphate the crossover analysis suggests adjustments for 20 cruises, as shown in Fig. 6. Deep  
281 phosphate measurements of 15 cruises (Table 6) appear to be lower than the respective reference  
282 measurements (i.e. phosphate data of these cruises require an increase), while the data of five cruises  
283 (#2, #3, #4, #6, #24) are higher (i.e. they need to be decreased) (Fig.3S). Applying all the indicated  
284 adjustments, the large offsets of cruises #2, #3, #4, #6, #8, #9, #10, #18, #20, #23 and #24 are reduced  
285 and become consistent with the reference. Cruises #1, #5, #12, #13, #14, #15, #16, #17, and #22 retain  
286 an offset even after applying the indicated adjustment. These cruises are considered in detail later.

287 According to Olsen et al. (2016), if a temporal trend is detected in the offsets, no adjustments should  
288 be applied. There is indeed a decreasing trend between 2008 and 2017 in the phosphate correction



289 factor (Fig. 6), and thus an increasing one in the weighted mean offset (Fig.3S), implying a temporal  
290 increase of phosphate. Therefore, phosphate data of the cruises being part of the trend were not  
291 flagged as questionable, except some cruises that are discussed further in section 5.4.

292 Comparing phosphate before and after adjustments, the corrections did minimise the difference with  
293 the reference, while the actual variation with time was preserved. The temporal trend towards higher  
294 phosphate concentrations in the Mediterranean Sea is considered to be real, even though studies  
295 concerning the biogeochemical trends in the deep layers of the WMED are scarce (Pasqueron et al.,  
296 2015). However this variation could be consistent with the findings of (Béthoux et al., 1998, 2002;  
297 Moon et al., 2016; Powley et al., 2018) modelling studies, who indeed found an increasing trend in  
298 phosphate concentrations over time.

### 299 **5.3 Silicate**

300 The results of the crossover analysis for silicate suggests corrections for all cruises (Fig.7). The  
301 crossovers indicate that deep silicate measurements are lower in the evaluated cruises than in the  
302 corresponding reference cruises (i.e. they need to be increased) (Fig.4S). This is likely to be a direct  
303 result of the samples freezing before analysis, since the reactive silica polymerizes when frozen  
304 (Becker et al., 2019). After applying the adjustment (Table 5), as expected, the offsets are reduced  
305 (Table 6), but five cruises (#1, #5, #6, #15, and #16) remain outside the accuracy envelope. Due to the  
306 large offsets, these cruises will be discussed further in section 5.4.

### 307 **5.4 Discussion and recommendation**

308 Adjustments were evaluated for each cruise separately. As a general rule no correction was applied  
309 when the suggested adjustment is strictly within the 2% limit (indicated with NA in Table 5). The  
310 average correction factors were 1.06 for nitrate, 1.14 for phosphate and 1.14 for silicate, respectively.  
311 To verify the results, we re-ran the crossover analysis and re-computed offsets and adjustment factors  
312 using the adjusted data (as shown in blue in Fig. 2S-3S-4S and Fig. 5-6-7). Most of the new



313 adjustments are within the accuracy envelope and only few are outside the limit, except for the cruises  
314 belonging to the above mentioned “phosphate-trend” and the other outlying cruises which are detailed  
315 hereafter.

316 Referring to the analysis detailed in section 4.2, the internal consistency of the nutrient data set has  
317 improved after the adjustment from 0.98% for nitrate, 0.83% for phosphate and 0.86% for silicate, to  
318 more unified dataset with 1.004 % for nitrate, 0.97 % for phosphate and 0.98% for silicate.

319 A comparison between the original and the adjusted vertical nutrient profiles is shown in Fig. 8,  
320 indicating an improvement in the accuracy based on the reference measurement and a relatively  
321 reduced range particularly for phosphate (Fig.8B). Figure 8.D-E scatterplots show that after the  
322 performed quality control, nutrient stoichiometry slopes obtained from regression, between tracers  
323 along the water column show a strong coupling and provide a nitrate to phosphate ratio of ~22.1 and  
324 nitrate to silicate ratio of ~0.94. These values are consistent with nutrient ratios range found in the  
325 WMED as reported in (Lazzari et al., 2016; Pujo-Pay et al., 2011; Segura-Noguera et al., 2016).

326 The regression model is more accurate after adjustments with an improved  $r^2$  for N:P from 0.81 to 0.90  
327 and for N:Si from 0.85 to 0.86.

328 Below we discuss the flags assigned in the adjusted dataset for some cruises that needed further  
329 consideration, since they required larger adjustment factors:

330 Cruise #1 [48UR20040526]: The adjusted values are still lower than the reference (Fig.5-6-7-Fig.2S-  
331 3S-4S) and are still outside the 2% accuracy range. This cruise had stations in the Sicily Channel,  
332 Tyrrhenian Sea and Corsica Channel (Fig. 9, right side) and only 4 stations were deeper than 1000 db  
333 (those within the Tyrrhenian Sea). The low precision of this cruise has already been evidenced during  
334 the primary QC (section 4.1). We recommend flagging this cruise as questionable.



335 Cruise #5 [48UR20051116]: This cruise took place between Sicily Channel and the Tyrrhenian Sea  
336 (Fig. 9, right side). Nitrate, phosphate and silicate data were lower than those from other cruises (#3  
337 and #4) run the same year (Fig. 5-6-7-Fig.2S-3S-4S) and are still biased after adjustments.  
338 Considering the limited precision and the low number of crossovers, it is recommended to flag the  
339 cruise as questionable.

340 Cruise #6 [48UR20060608]: The silicate bias was reduced after adjustment but remains large with  
341 respect to the accuracy limit (Fig. 7-Fig. 4S). This cruise has a wide geographic coverage, with  
342 stations along 9 sections (Fig. 9, right side). Considering also the high standard deviation (Table 3),  
343 which is partially attributed to the spatial coverage of the cruise, there still remains uncertainty about  
344 the quality of the samples. It is recommended to flag silicate data of cruise #6 as questionable.

345 Cruise #12 [48UR20081103]: Phosphate data have low accuracy with respect to the reference cruises  
346 (Fig. 6-Fig. 3S). This cruise has stations along a longitudinal section from the Sicily Channel to the  
347 Gibraltar Strait, which might explain the large standard deviation of deep phosphate samples (Table  
348 3). In addition, considering the relatively high number of stations >1000 db and a plausible trend in  
349 phosphate, it is not recommended to flag the phosphate data as questionable.

350 Cruise #15 [48UR20100731]: This cruise had 149 station along a similar track as cruise #12 and  
351 shows large offsets for phosphate and silicate (Fig. 6-7-Fig. 3S-4S), compared to cruise #12.  
352 Considering that deep silicate data was not of low quality (small standard deviation, see Table 3), and  
353 that deep phosphate fall within the “phosphate-trend” discussed above, we do not recommend flagging  
354 as questionable.

355 Cruise #16 [48UR20101123]: The cruise shows large offsets for phosphate and silicate (Fig. 6-7- Fig.  
356 3S-4S), similar to cruise #15. Considering that the standard deviation of silicate samples below 1000  
357 db was relatively high (1.02 over 14 samples, see Table 3), and that it has only one crossover (Table  
358 6), it is recommended to flag silicate data of cruise #16 as questionable. As for phosphate, the cruise is  
359 part of the “phosphate-trend” and is therefore not recommended to be flagged as questionable.



360 Cruise #24 [48QL20171023]: This cruise has the largest offset for nitrate even after adjustment. It is  
361 very likely due to a difference between laboratories (calibration standards) concerning nitrate, which  
362 needs to be flagged as questionable.

363 Cruises discussed in this section were not removed from the final product but are retained along with  
364 their quality flags detailed above. We have done the evaluation of their overall quality but leave it up  
365 to the users how to appropriately use these data.

## 366 **6 Final remarks**

367 An internally consistent data set of dissolved inorganic nutrients has been generated for the WMED  
368 (2004-2017). The accuracy envelope for nitrate and silicate was set to ~2%, a predefined limit used in  
369 GLODAP and CARINA datasets. Regarding phosphate data, these were almost entirely outside this  
370 limit, because of its natural variations and overall very low concentrations in the WMED, a highly P-  
371 limited basin. Using a crossover analysis to compare cruises with respect to reference data, improved  
372 the accuracy of the measurements by bias-minimizing the individual cruises.

373 The publication of a quality-controlled extensive (spatially and temporally) database of inorganic  
374 nutrients in the WMED was timely, and fills a gap in information that prevented baseline assessments  
375 on spatial and temporal variability of biogeochemical tracers in the Mediterranean. In combination  
376 with older databases in the same region (e.g. bottle data available in the MEDAR/MEDATLAS  
377 database), this new database will thus constitute a pillar on which the Mediterranean marine scientific  
378 community will be able to build on original research topics on biogeochemical fluxes and cycles and  
379 their relation to hydrological changes that occurred in the period covered by the dataset. The dataset is  
380 also relevant for the modelling community as it can be used as an independent dataset to assess  
381 reanalysis product or it can be assimilated in new reanalysis products.

## 382 **7 Data availability**





383 The final dataset is available as a .csv files from PANGAEA, and can be accessed at  
384 <https://doi.pangaea.de/10.1594/PANGAEA.904172> (Belgacem et al. 2019).

385 Ancillary information is in the supplementary materials with the list of variables included in original  
386 and final product. Table 1 summarizes all cruises included in the dataset. The dataset include  
387 frequently measured stations and key transects of the WMED with in situ physical and chemical  
388 oceanographic observations. As mentioned, two files are accessible, both include oceanographic  
389 variables observed at the standard depths (see supplementary materials Part-2).

390 - *Original dataset: CNR\_DIN\_WMED\_20042017\_original.csv*: This is the original dataset with  
391 flag variable for each of the following parameter: CTD salinity, nitrate, phosphate and silicate  
392 from the primary quality control (detailed in section 4.1).

393 - *Adjusted dataset: CNR\_DIN\_WMED\_20042017\_adjusted.csv*: This is the product after  
394 primary quality control and after applying the adjustment factors from the secondary quality  
395 control. Recommendations of section 5.4 are included, as well as quality flags.

396 **Author contribution:** MB, MA, SL, JC and KS substantially contributed to write the manuscript. SC,  
397 GC and FA run the chemical analysis and contributed to the manuscript. MB coordinated the technical  
398 aspects of most of the cruises. SC, GC, FA, AR, BP contributed in specific part of the manuscript.

399 **Acknowledgements.** The data have been collected in the framework of several of national and  
400 European projects, e.g.: KM3NeT, EU GA #011937; SESAME, EU GA #GOCE-036949; PERSEUS,  
401 EU GA #287600; OCEAN-CERTAIN, EU GA #603773; COMMON SENSE, EU GA #228344;  
402 EUROFLEETS, EU GA #228344; EUROFLEETS2, EU GA # 312762; JERICO, EU GA #262584;  
403 the Italain PRIN 2007 program “Tyrrhenian Seamounts ecosystems”, and the Italian RITMARE  
404 Flagship Project, both funded by the Italian Ministry of University and Research. We thank Sarah  
405 Jutterström from the Swedish Environmental Research institute for the invaluable help in Quality  
406 Control discussions. We would like to express our appreciation to the laboratory team at IEO for their



407 help and collaboration during MB's stay there. The authors are deeply indebted to all investigators and  
408 analysts who contributed to data collection at sea during so many years, as well as to the PIs of the  
409 cruises (S. Aliani, M. Astraldi, M. Azzaro, M. Dibitto, G. P. Gasparini, A. Griffa, J. Haun, L. Jullion,  
410 G. La Spada, E. Manini, A. Perilli, C. Santinelli, S. Sparnocchia), the captains and the crews for  
411 allowing the collection of this enormous dataset; without them, this work would not have been  
412 possible.

413

414

415

416

417

418

419

420

421

422

#### 423 **References**

424 Aoyama, M., Woodward, E. Malcolm S. Bakker, K., Becker, S., Björkman, K., Daniel, A., Mahaffey,  
425 C., Murata, A., Naik, H., Tanhua, T., Rho, T., Roman, R. and Sloyan, B.: Comparability of oceanic  
426 nutrient data., 2016.

427 Becker, S., Aoyama, M., Woodward, E. M. S., Bakker, K. and Coverly, S.: GO-SHIP Repeat  
428 Hydrography Nutrient Manual , 2019 : The precise and accurate determination of dissolved inorganic  
429 nutrients in seawater ; Continuous Flow Analysis methods and laboratory practices ., , 49, 2019.



- 430 Belgacem, M., Chiggiato, J., Borghini, M., Pavoni, B., Cerrati, G., Acri, F; Cozzi, S., Ribotti, A.,  
431 Álvarez, M., Lauvset, S. K., Schroeder, K. (2019): Quality controlled dataset of dissolved inorganic  
432 nutrients in the western Mediterranean Sea (2004-2017) from R/V oceanographic cruises. PANGAEA,  
433 <https://doi.pangaea.de/10.1594/PANGAEA.904172>
- 434 Bethoux, J. P.: Oxygen consumption, new production, vertical advection and environmental evolution  
435 in the Mediterranean Sea, *Deep Sea Res. Part A, Oceanogr. Res. Pap.*, 36(5), 769–781,  
436 doi:10.1016/0198-0149(89)90150-7, 1989.
- 437 Bethoux, J. P., Morin, P., Madec, C. and Gentili, B.: Phosphorus and nitrogen behaviour in the  
438 Mediterranean Sea, *Deep Sea Res. Part A, Oceanogr. Res. Pap.*, 39(9), 1641–1654, doi:10.1016/0198-  
439 0149(92)90053-V, 1992.
- 440 Bethoux, J. P., Gentili, B., Morin, P., Nicolas, E., Pierre, C. and Ruiz-Pino, D.: The Mediterranean  
441 Sea : a miniature ocean for climatic and environmental studies and a key for the climatic functioning of  
442 the North Atlantic, *Prog. Oceanogr.*, 44, 131–146, 1999.
- 443 Béthoux, J. P., Morin, P., Chaumery, C., Connan, O., Gentili, B. and Ruiz-Pino, D.: Nutrients in the  
444 Mediterranean Sea, mass balance and statistical analysis of concentrations with respect to  
445 environmental change, *Mar. Chem.*, 63(1–2), 155–169, doi:10.1016/S0304-4203(98)00059-0, 1998.
- 446 Béthoux, J. P., Morin, P. and Ruiz-Pino, D. P.: Temporal trends in nutrient ratios: Chemical evidence  
447 of Mediterranean ecosystem changes driven by human activity, *Deep. Res. Part II Top. Stud.*  
448 *Oceanogr.*, 49(11), 2007–2016, doi:10.1016/S0967-0645(02)00024-3, 2002.
- 449 Boyd, P. W.: Beyond ocean acidification, *Nat. Geosci.*, 4(5), 273–274, doi:10.1038/ngeo1150, 2011.
- 450 Dickson, A. G., Afghan, J. D. and Anderson, G. C.: Reference materials for oceanic CO<sub>2</sub> analysis: A  
451 method for the certification of total alkalinity, *Mar. Chem.*, 80(2–3), 185–197, doi:10.1016/S0304-  
452 4203(02)00133-0, 2003.
- 453 Fichaut, M., Garcia, M. J., Giorgetti, A., Iona, A., Kuznetsov, A., Rixen, M. and Group, M.:  
454 MEDAR/MEDATLAS 2002: A Mediterranean and Black Sea database for operational oceanography,  
455 *Elsevier Oceanogr. Ser.*, 69, 645–648, doi:10.1016/S0422-9894(03)80107-1, 2003.
- 456 Giorgi, F.: Climate change hot-spots, *Geophys. Res. Lett.*, 33(8), 1–4, doi:10.1029/2006GL025734,  
457 2006.
- 458 Gouretski, V. V. and Jancke, K.: Systematic errors as the cause for an apparent deep water property  
459 variability: Global analysis of the WOCE and historical hydrographic data, *Prog. Oceanogr.*, 48(4),  
460 337–402, doi:10.1016/S0079-6611(00)00049-5, 2001.
- 461 Grasshoff, K., Kremling K., Ehrhardt M.: *Methods of seawater analysis* (3rd ed.), Weinheim  
462 Press, WILEY-VCH, 203-273, 1999.  
463
- 464 Hansen, H. P. and Koroleff, F.: Chapter 10: Determination of nutrients, *Methods Seawater Anal.*, 159–  
465 228, 1999.
- 466 Hoppema, M., Velo, A., van Heuven, S., Tanhua, T., Key, R. M., Lin, X., Bakker, D. C. E., Perez, F.  
467 F., Ríos, A. F., Lo Monaco, C., Sabine, C. L., Álvarez, M. and Bellerby, R. G. J.: Consistency of  
468 cruise data of the CARINA database in the Atlantic sector of the Southern Ocean, *Earth Syst. Sci.*  
469 *Data*, 1(1), 63–75, doi:10.5194/essd-1-63-2009, 2009.



- 470 Johnson, G. C., Robbins, P. E. and Hufford, G. E.: Systematic adjustments of hydrographic sections  
471 for internal consistency, *J. Atmos. Ocean. Technol.*, 18(7), 1234–1244, doi:10.1175/1520-  
472 0426(2001)018<1234:SAOHSF>2.0.CO;2, 2001.
- 473 Key, R. M., Kozyr, A., Sabine, C. L., Lee, K., Wanninkhof, R., Bullister, J. L., Feely, R. A., Millero,  
474 F. J., Mordy, C. and Peng, T. H.: A global ocean carbon climatology: Results from Global Data  
475 Analysis Project (GLODAP), *Global Biogeochem. Cycles*, 18(4), 1–23, doi:10.1029/2004GB002247,  
476 2004.
- 477 Lauvset, S. K. and Tanhua, T.: A toolbox for secondary quality control on ocean chemistry and  
478 hydrographic data, *Limnol. Oceanogr. Methods*, 13(11), 601–608, doi:10.1002/lom3.10050, 2015.
- 479 Lazzari, P., Solidoro, C., Salon, S. and Bolzon, G.: Spatial variability of phosphate and nitrate in the  
480 Mediterranean Sea: A modeling approach, *Deep. Res. Part I*, 108, 39–52,  
481 doi:10.1016/j.dsr.2015.12.006, 2016.
- 482 Lejeusne, C., Chevaldonné, P., Pergent-Martini, C., Boudouresque, C. F. and Pérez, T.: Climate  
483 change effects on a miniature ocean: the highly diverse, highly impacted Mediterranean Sea, *Trends*  
484 *Ecol. Evol.*, 25(4), 250–260, doi:10.1016/j.tree.2009.10.009, 2010.
- 485 Moon, J., Lee, K., Tanhua, T., Kress, N. and Kim, I.: Temporal nutrient dynamics in the  
486 Mediterranean Sea in response to anthropogenic inputs, , 5243–5251,  
487 doi:10.1002/2016GL068788.Received, 2016.
- 488 Muniz, K., Cruzado, A., Ruiz De Villa, C. and Villa, C. R. De: Statistical analysis of nutrient data  
489 quality ( nitrate and phosphate ), applied to useful predictor models in the northwestern Mediterranean  
490 Sea, *Methodology*, 17, 221–231, 2001.
- 491 Olsen, A., Key, R. M., Heuven, S. Van, Lauvset, S. K., Velo, A., Lin, X., Schirnack, C., Kozyr, A.,  
492 Tanhua, T., Hoppema, M. and Jutterström, S.: The Global Ocean Data Analysis Project version 2 (  
493 GLODAPv2 ) – an internally consistent data product for the world ocean, , 297–323,  
494 doi:10.5194/essd-8-297-2016, 2016.
- 495 Pasqueron, O., Fommervault, D., Migon, C., Ortenzio, F. D., Ribera, M. and Coppola, L.: Deep-Sea  
496 Research I Temporal variability of nutrient concentrations in the northwestern Mediterranean sea (  
497 DYFAMED time-series station ), *Deep. Res. Part I*, 100, 1–12, doi:10.1016/j.dsr.2015.02.006, 2015.
- 498 Powley, H. R., Krom, M. D. and Van Cappellen, P.: Phosphorus and nitrogen trajectories in the  
499 Mediterranean Sea (1950–2030): Diagnosing basin-wide anthropogenic nutrient enrichment, *Prog.*  
500 *Oceanogr.*, 162, 257–270, doi:10.1016/j.pocean.2018.03.003, 2018.
- 501 Pujo-Pay, M., Conan, P., Oriol, L., Cornet-Barthaux, V., Falco, C., Ghiglione, J. F., Goyet, C.,  
502 Moutin, T. and Prieur, L.: Integrated survey of elemental stoichiometry (C, N, P) from the western to  
503 eastern Mediterranean Sea, *Biogeosciences*, 8(4), 883–899, doi:10.5194/bg-8-883-2011, 2011.
- 504 Sabine, C. L., Hoppema, M., Key, R. M., Tilbrook, B., Van Heuven, S., Lo Monaco, C., Metzl, N.,  
505 Ishii, M., Murata, A. and Musielewicz, S.: Assessing the internal consistency of the CARINA data  
506 base in the Pacific sector of the Southern Ocean, *Earth Syst. Sci. Data*, 2(2), 195–204,  
507 doi:10.5194/essd-2-195-2010, 2010.
- 508 Schroeder, K., Tanhua, T., Bryden, H., Alvarez, M., Chiggiato, J. and Aracri, S.: Mediterranean Sea  
509 Ship-based Hydrographic Investigations Program (Med-SHIP), *Oceanography*, 28(3), 12–15,  
510 doi:10.5670/oceanog.2015.71, 2015.



- 511 Schroeder, K., Chiggiato, J., Bryden, H. L., Borghini, M. and Ismail, S. Ben: Abrupt climate shift in  
512 the Western Mediterranean Sea, *Nat. Publ. Gr.*, 1–7, doi:10.1038/srep23009, 2016.
- 513 Segura-Noguera, M., Cruzado, A. and Blasco, D.: The biogeochemistry of nutrients, dissolved oxygen  
514 and chlorophyll a in the Catalan Sea (NW Mediterranean Sea), *Sci. Mar.*, 80(S1), 39–56,  
515 doi:10.3989/scimar.04309.20a, 2016.
- 516 Suzuki, T., Ishii, M., Aoyama, A., Christian, J. R., Enyo, K., Kawano, T., Key, R. M., Kosugi, N.,  
517 Kozyr, A., Miller, L. A., Murata, A., Nakano, T., Ono, T., Saino, T., Sasaki, K., Sasano, D., Takatani,  
518 Y., Wakita, M., and Sabine, C. L.: PACIFICA Data Synthesis Project, ORNL/CDIAC-159, NDP-092,  
519 Carbon Dioxide Information Analysis Center, Oak Ridge National Laboratory, U. S. Department of  
520 Energy, Oak Ridge, Tennessee, 2013.
- 521 Tanhua, Toste (2019): Hydrochemistry of water samples during MedSHIP cruise Talpro. PANGAEA,  
522 <https://doi.org/10.1594/PANGAEA.902293>.
- 523 Tanhua, T.: Matlab Toolbox to Perform Secondary Quality Control (2nd QC) on Hydrographic Data,  
524 ORNL CDIAC-158. Carbon Dioxide Inf. Anal. Center, Oak Ridge Natl. Lab. U.S. Dep. Energy, Oak  
525 Ridge, Tennessee, 158, doi:10.3334/CDIAC/otg.CDIAC\_158, 2010a.
- 526 Tanhua, T., Brown, P. J. and Key, R. M.: Science Data CARINA : nutrient data in the Atlantic Ocean,  
527 *Earth*, 1, 7–24, doi:10.3334/CDIAC/otg.CARINA.ATL.V1.0, 2009.
- 528 Tanhua, T., Heuven, S. van, Key, R. M., Velo, A., Olsen, A. and Schirnick, C.: Quality control  
529 procedures and methods of the CARINA database, *Earth Syst. Sci. Data*, 2, 35–49, 2010b.
- 530 Tanhua, T., Hainbucher, D., Schroeder, K., Cardin, V., Álvarez, M. and Civitarese, G.: The  
531 Mediterranean Sea system: A review and an introduction to the special issue, *Ocean Sci.*, 9(5), 789–  
532 803, doi:10.5194/os-9-789-2013, 2013.
- 533 Testor, P., Bosse, A., Houpert, L., Margirier, F., Mortier, L., Legoff, H., Dausse, D., Labaste, M.,  
534 Karstensen, J., Hayes, D., Olita, A., Ribotti, A., Schroeder, K., Chiggiato, J., Onken, R., Heslop, E.,  
535 Mourre, B., D’ortenzio, F., Mayot, N., Lavigne, H., de Fommervault, O., Coppola, L., Prieur, L.,  
536 Taillandier, V., Durrieu de Madron, X., Bourrin, F., Many, G., Damien, P., Estournel, C., Marsaleix,  
537 P., Taupier-Letage, I., Raimbault, P., Waldman, R., Bouin, M. N., Giordani, H., Caniaux, G., Somot,  
538 S., Ducrocq, V. and Conan, P.: Multiscale Observations of Deep Convection in the Northwestern  
539 Mediterranean Sea During Winter 2012–2013 Using Multiple Platforms, *J. Geophys. Res. Ocean.*,  
540 123(3), 1745–1776, doi:10.1002/2016JC012671, 2018.
- 541
- 542
- 543
- 544
- 545
- 546
- 547



548 **Figure Captions**

549 **Figure 1.** Map of the Western Mediterranean Sea showing the biogeochemical stations (in blue) and  
550 the five reference cruise stations (in red).

551 **Figure 2.** Overview of the reference cruise spatial coverage and vertical distributions of the inorganic  
552 nutrients. Top left: geographical distribution map, top right: vertical profiles of nitrate in  $\mu\text{mol kg}^{-1}$ ,  
553 bottom left: vertical profiles of phosphate in  $\mu\text{mol kg}^{-1}$ , bottom right: vertical profiles of silicate in  
554  $\mu\text{mol kg}^{-1}$ .

555 **Figure 3.** Scatter plots of (A.) phosphate vs nitrate (in  $\mu\text{mol kg}^{-1}$ ) and (B.) silicate vs. nitrate (in  $\mu\text{mol}$   
556  $\text{kg}^{-1}$ ). Data that have been flagged as “questionable” (flag=3) are in red, the colour bar indicates the  
557 pressure (in dbar). The black lines represent the best linear fit between the two parameters, and the  
558 corresponding equations and  $r^2$  values are shown on each plot. Average resulting N:P ratio is 20.91,  
559 average resulting N:Si ratio is 1.05 (whole depth).

560 **Figure 4.** An example of the calculated offset for silicate between cruise 48UR20131015 and cruise  
561 29AJ2016818 (reference cruise). Above: location of the stations being part of the crossover and  
562 statistics. Bottom left: vertical profiles of silicate data in ( $\mu\text{mol kg}^{-1}$ ) of the two cruises that fall within  
563 the minimum distance criteria (the crossing region), below 1000 dbar. Bottom right: vertical plot of  
564 the difference between both cruises (dotted black line) with standard deviations (dashed black lines)  
565 and the weighted average of the offset (solid red line) with the weighted standard deviations (dotted  
566 red line).

567 **Figure 5.** Results of the crossover analysis for nitrate, before (grey) and after adjustment (blue). Error  
568 bars indicate the standard deviation of the absolute weighted offset. The dashed lines indicate the  
569 accuracy limit 2% for an adjustment to be recommended.

570 **Figure 6.** The same as Fig. 5 but for phosphate.



571 **Figure 7.** The same as Fig. 5 but for silicate.

572 **Figure 8.** Dataset comparison before (black) and after (blue) adjustment, showing vertical profiles of  
573 (A.) nitrate (in  $\mu\text{mol kg}^{-1}$ ), (B.) phosphate (in  $\mu\text{mol kg}^{-1}$ ) and (C.) silicate (in  $\mu\text{mol kg}^{-1}$ ). Scatter plots  
574 of the adjusted data from all depths after 1<sup>st</sup> and 2<sup>nd</sup> quality control for (D.) phosphate vs nitrate (in  
575  $\mu\text{mol kg}^{-1}$ ) and (E.) silicate vs. nitrate (in  $\mu\text{mol kg}^{-1}$ ). The black lines represent the best linear fit  
576 between the two parameters, and the corresponding equations and  $r^2$  values are shown on each plot.  
577 Average resulting N:P ratio is 22.17, average resulting N:Si ratio is 0.94 (whole depth).

578 **Figure 9.** Vertical profiles of the inorganic nutrients in the dataset after adjustments and spatial  
579 coverage of each cruise (reference to cruise ID is above each map). The whole WMED adjusted  
580 dataset is shown in black while the data of each individual cruise are shown in blue (flag=2) and green  
581 (flag=3).

582



583 **Table captions**

584 **Table 1.** Cruise summary table and parameters listed with number of stations and samples. Cruises  
585 were identified with an ID number and expedition code ('EXPOCODE' of format  
586 AABBYYYMMDD with AA: country code, BB: ship code, YYYY: year, MM: month, DD: day  
587 indicative of cruise starting day)

588 **Table 2.** Cruise summary table of the reference cruises collection used in the secondary quality  
589 control, collected from 2001 to 2016.

590 **Table 3.** WOCE flags used in the original data product.

591 **Table 4.** Standard deviations of nitrate, phosphate and silicate measurements with number of samples  
592 deeper than 1000db included in the 2<sup>nd</sup> QC. Storage time: the minimum storage time defined as time  
593 difference between the cruise ending day and the 1<sup>st</sup> day of the laboratory analysis

594 **Table 5.** Summary of the suggested adjustment for nitrate, phosphate and silicate resulting from the  
595 crossover analysis. Adjustments for inorganic nutrient are multiplicative. NA: denotes not adjusted,  
596 i.e. data of cruises that could not be used in the crossover analysis, because of the lack of stations or  
597 data are outside the spatial coverage of reference cruises.

598 **Table 6.** Secondary QC toolbox results: improvements of the weighted mean of absolute offset per  
599 cruise of unadjusted and adjusted data; (n) is the number of crossovers per cruise. The numbers in red  
600 (less than 1) indicate that the cruise data are lower than the reference cruises. NA: not adjusted.

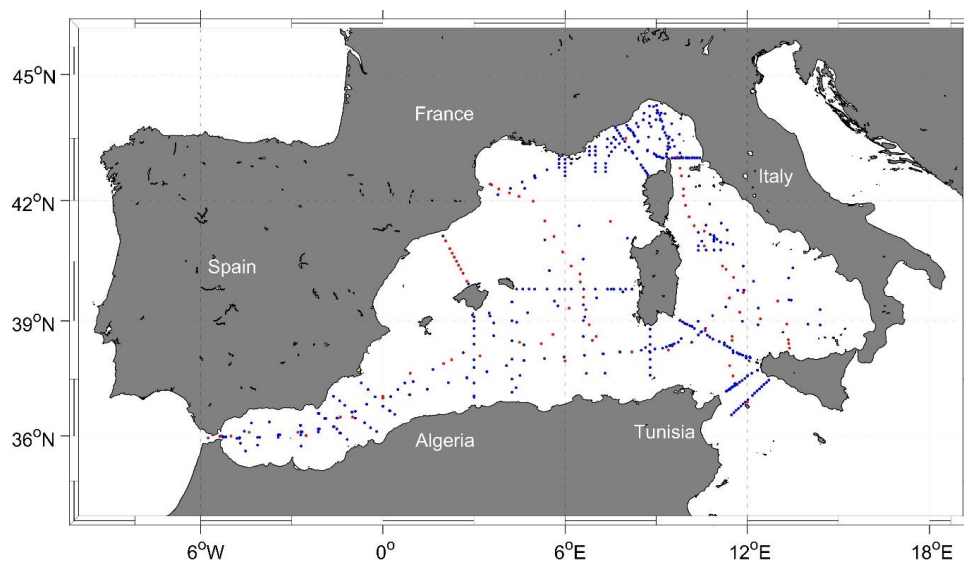
601





602 **Figure 1**

603



604

605

606

607

608

609

610

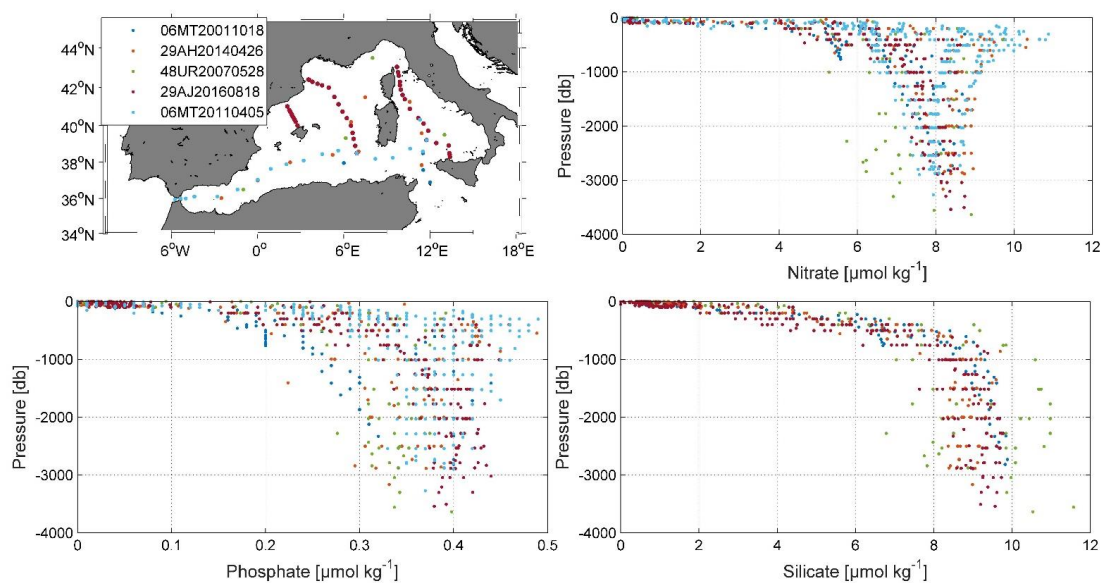
611

612

613



614 **Figure 2**



615

616

617

618

619

620

621

622

623

624

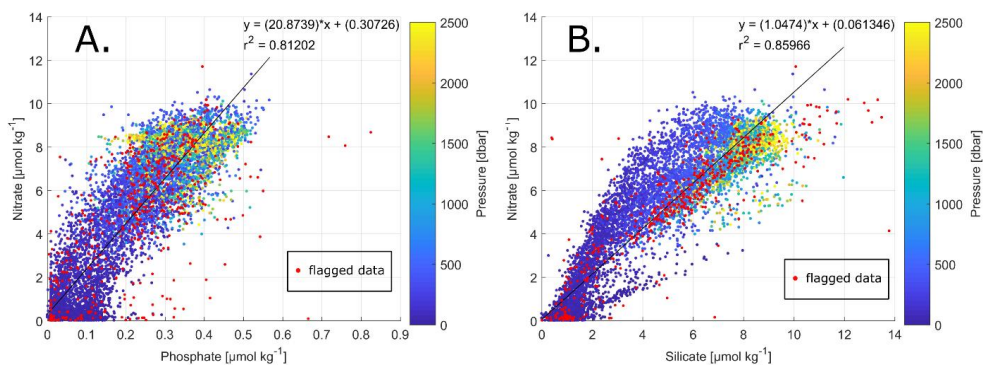
625

626

627



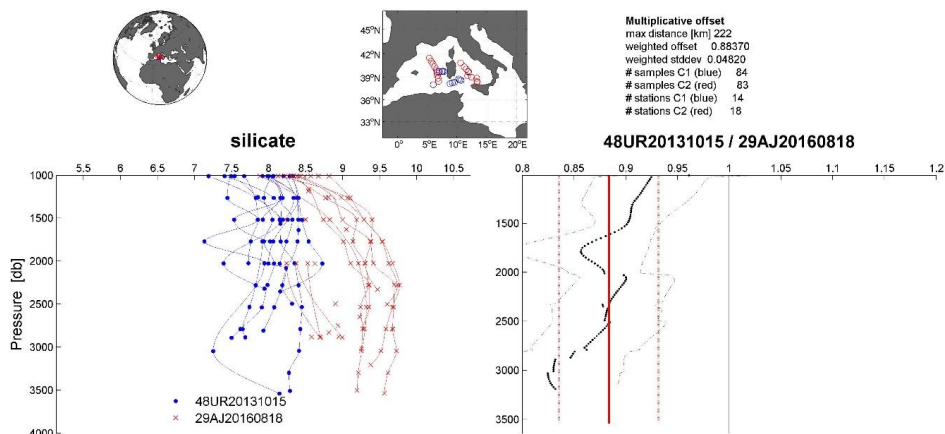
628 **Figure 3**



629

630

631 **Figure 4**



632

633

634

635

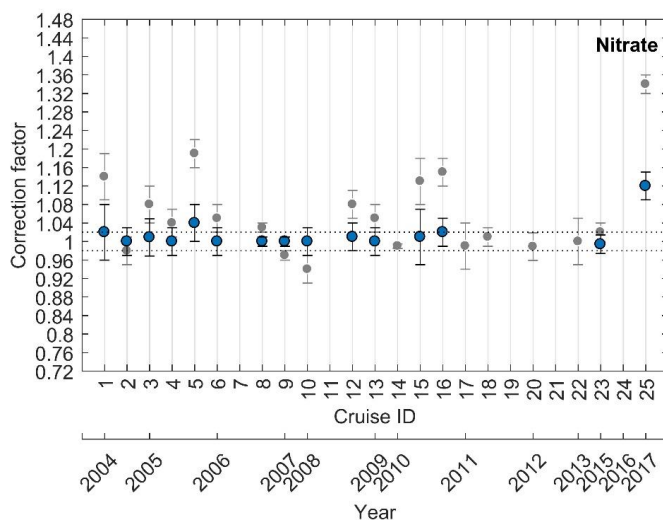
636

637

638



639 **Figure 5**



640

641

642

643

644

645

646

647

648

649

650

651

652

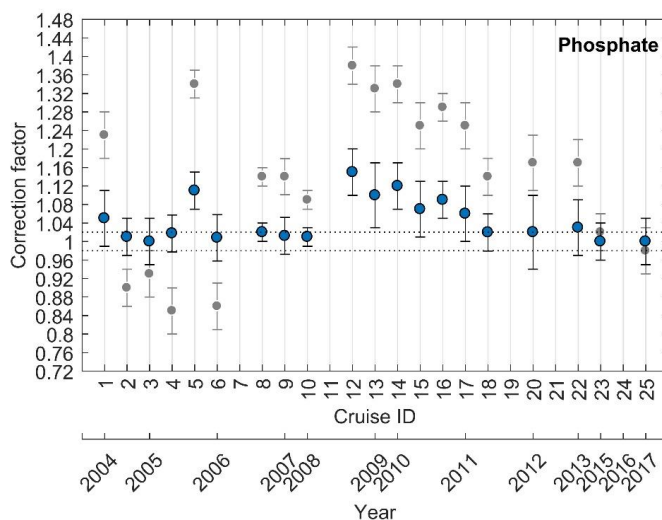
653

654

655



656 **Figure 6**



657

658

659

660

661

662

663

664

665

666

667

668

669

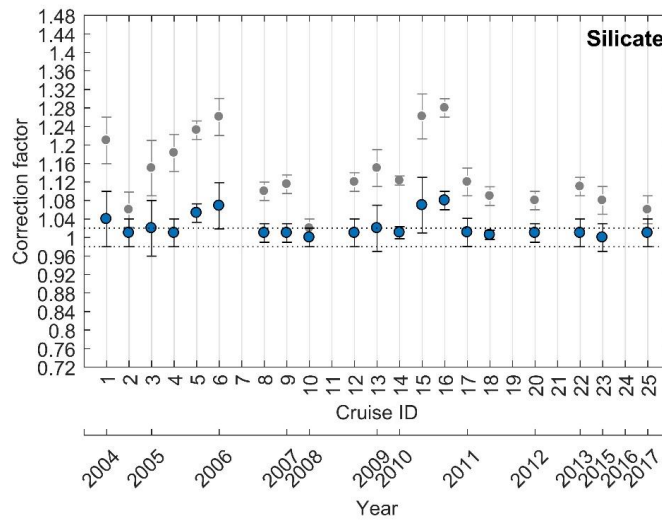
670

671

672



673 **Figure 7**



674

675

676

677

678

679

680

681

682

683

684

685

686

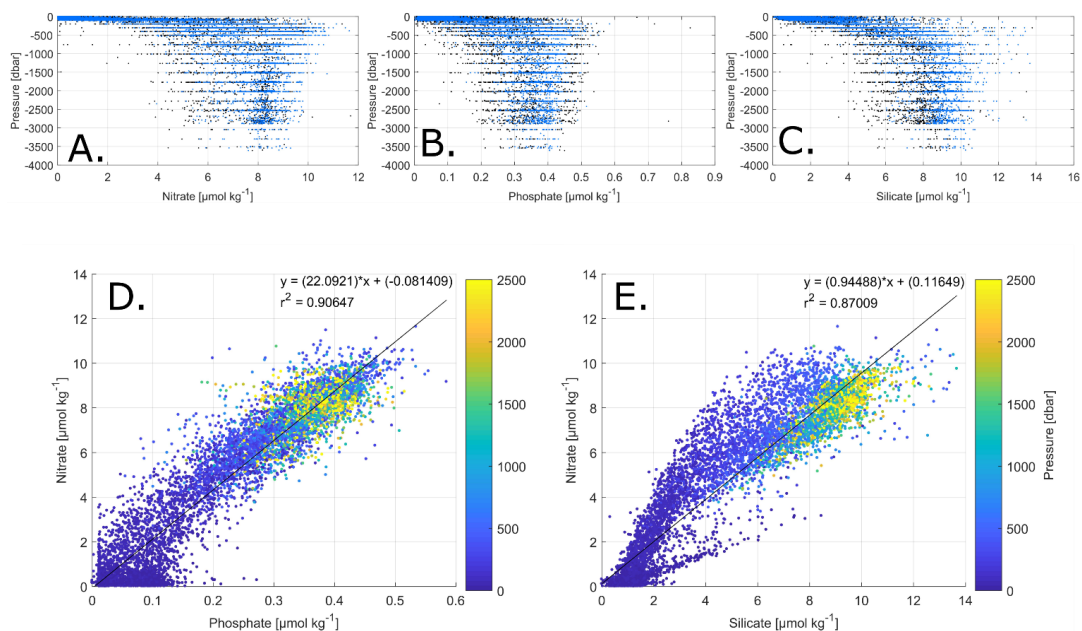
687

688

689



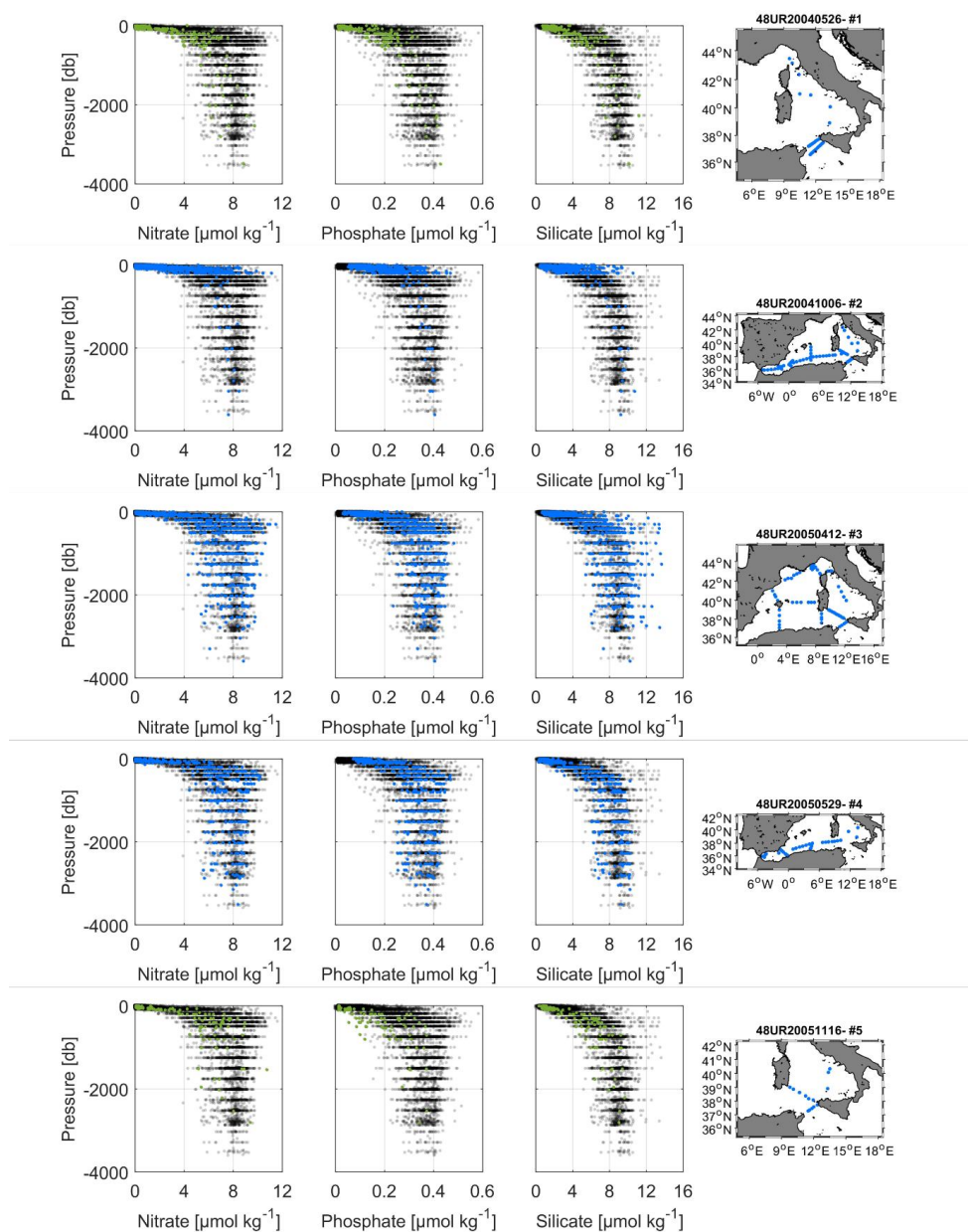
690 **Figure 8**



691  
692  
693  
694  
695  
696  
697  
698  
699  
700  
701  
702  
703  
704

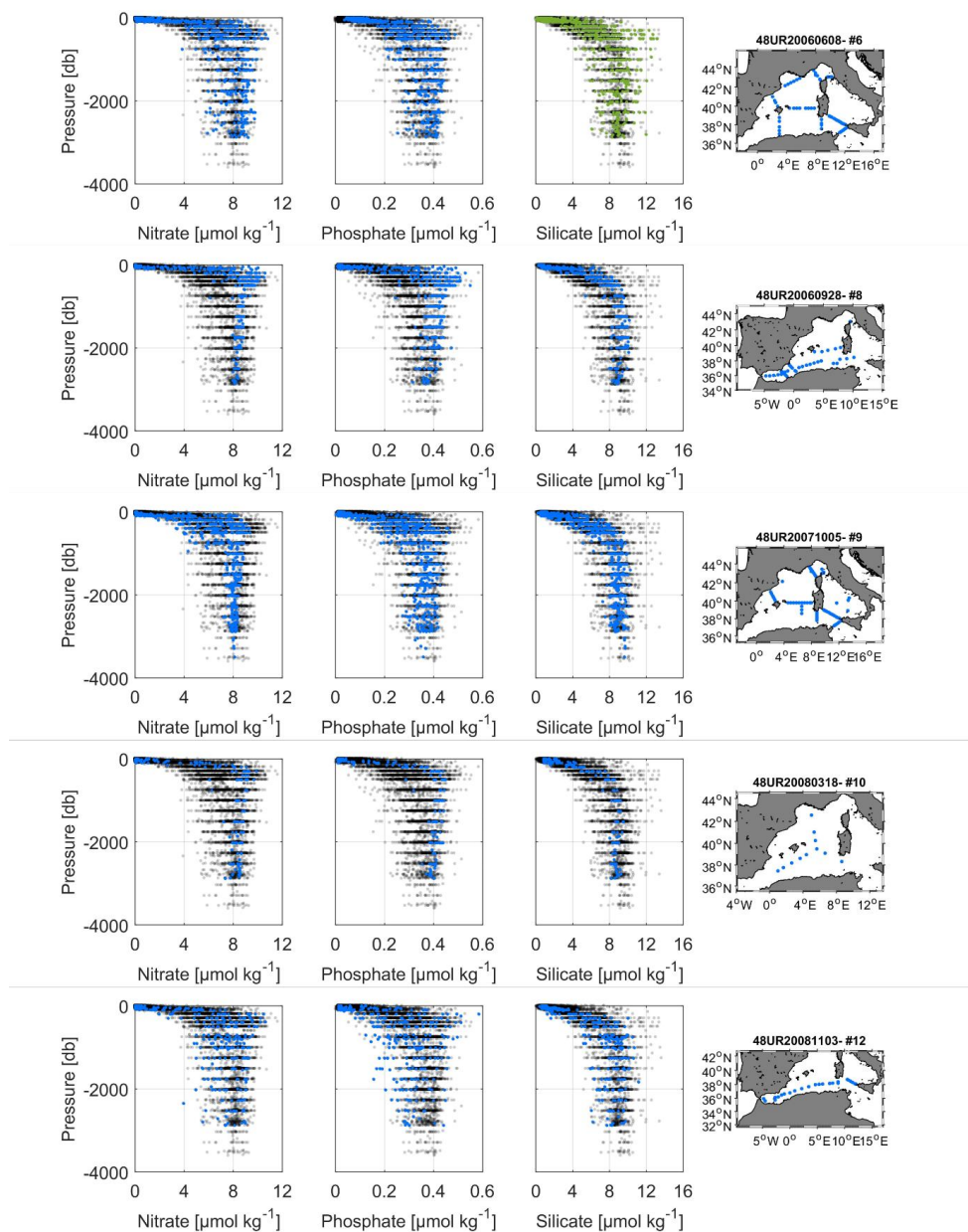


705 **Figure 9**



706

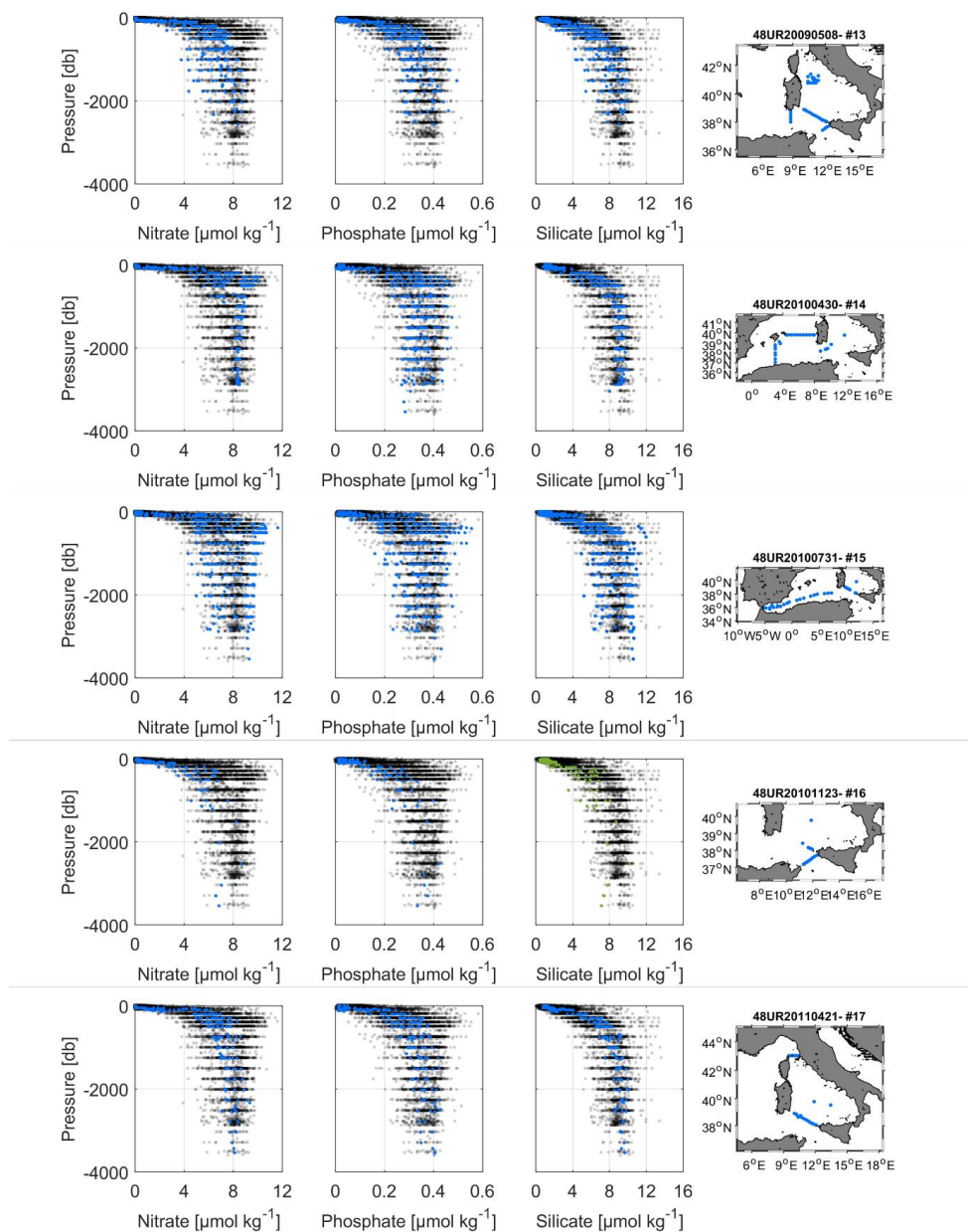




707

708

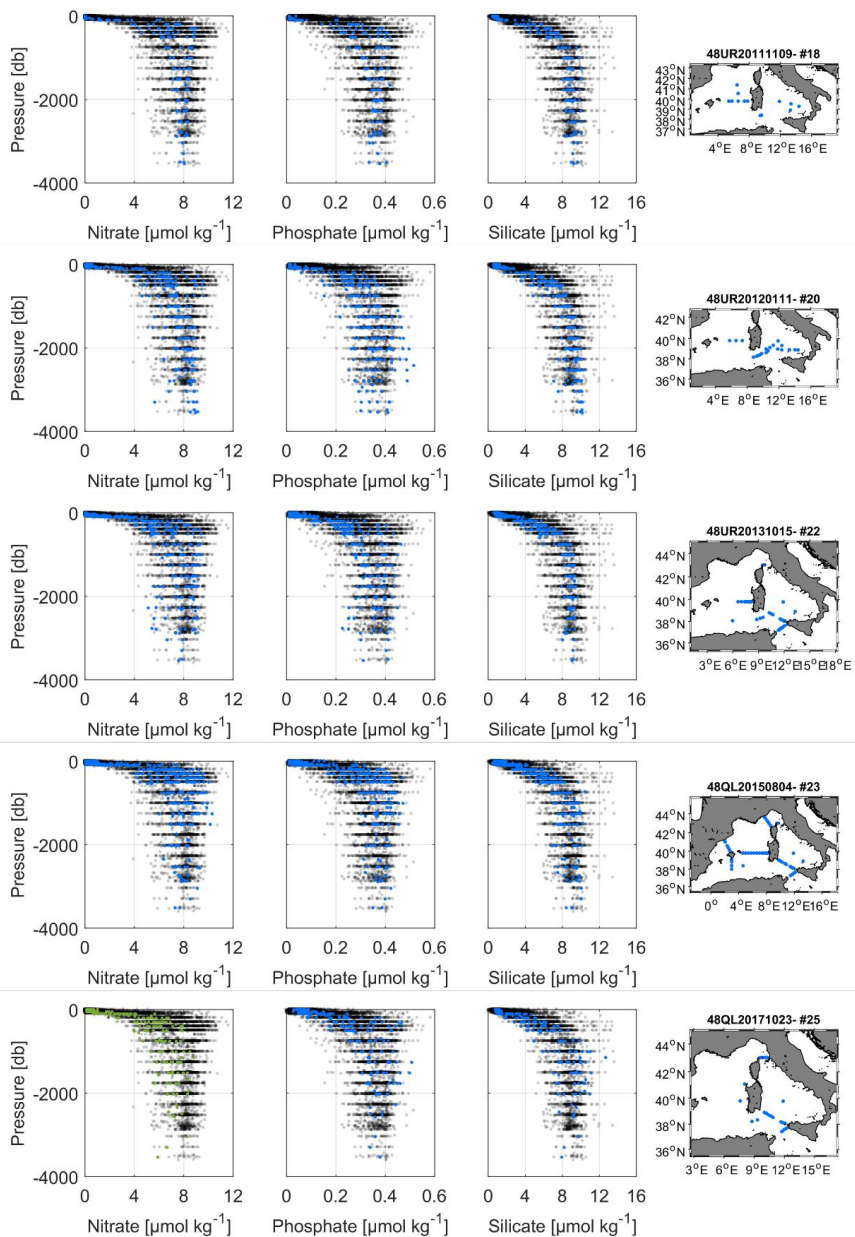
709



710

711

712



713

714

715

716



**Table 1**

Cruise ID (#)	Common Name	EXPOCODE	Research vessel	Date Start/End	Stations	Samples NO <sub>3</sub>	Samples PO <sub>4</sub>	Samples SiO <sub>2</sub>	Maximum bottom depth (m)	Chief scientist
1	TRENDS2004/MEDGOOS8leg2	48UR20040526	Urania	26 MAY - 14 JUN 2004	36	255	253	255	3499	M. Borghini
2	MEDGOOS9	48UR20041006	Urania	6 - 25 OCT 2004	68	627	626	627	3610	M. Borghini
3	MEDOC05/MFSTEP2	48UR20050412	Urania	12 APR - 16 MAY 2005	68	828	828	828	3598	M. Borghini
4	MEDGOOS10	48UR20050529	Urania	29 MAY - 10 JUN 2005	36	577	577	577	3505	A. Perilli
5	MEDGOOS11	48UR20051116	Urania	16 NOV - 3 DEC 2005	14	143	143	143	2810	A. Perilli, M. Borghini, M. Dibitetto
6	MEDOC06	48UR20060608	Urania	8 JUN - 3 JUL 2006	66	787	785	787	2881	M. Borghini
7	SIRENA06	06A420060720	NRV Alliance	20 JUL - 6 AUG 2006	35	208	208	209	1854	J. Haun
8	MEDGOOS13/MEDBIO06	48UR20060928	Urania	28 SEP - 8 NOV 2006	37	519	520	520	2862	A. Ribotti
9	MEDOC07	48UR20071005	Urania	5 - 29 OCT 2007	71	977	977	979	3497	A. Perilli
10	SESAMEI4	48UR20080318	Urania	18 MAR - 7 APR 2008	11	164	164	164	2882	C. Santinelli
11	SESAMEI5	48UR20080905	Urania	5 - 16 SEP 2008	12	74	74	74	536	S. Sparnocchia, G.P. Gasparini, M. Borghini
12	MEDCO08	48UR20081103	Urania	3 - 24 NOV 2008	24	342	350	348	2880	A. Ribotti
13	TYRRMOUNTS	48UR20090508	Urania	8 MAY - 3 JUN 2009	41	430	441	440	2559	G.P. Gasparini
14	BIOFUN010	48UR20100430	Urania	30 APR - 17 MAY 2010	26	405	405	405	3540	E. Mammi, S. Aliani
15	VENUS1	48UR20100731	Urania	31 JUL - 25 AUG 2010	32	431	432	428	3544	G.P. Gasparini, M. Borghini
16	BONSI02010	48UR20101123	Urania	23 NOV - 9 DEC 2010	18	144	143	143	3540	A. Ribotti
17	EUROFLEET11	48UR20110421	Urania	21 APR - 8 MAY 2011	28	277	275	277	3540	G.P. Gasparini, M. Borghini
18	BONIFAGIO2011	48UR20111109	Urania	9 - 23 NOV 2011	13	180	180	181	3541	A. Ribotti, G. La Spada, M. Borghini
19	TOSCA2011	48MG20111210	Maria Grazia	10 - 20 DEC 2011	21	310	310	309	2728	M. Borghini
20	ICHNUSSA12	48UR20120111	Urania	11 - 27 JAN 2012	21	353	352	323	3551	A. Ribotti
21	EUROFLEET2012	48UR20121108	Urania	8 - 26 NOV 2012	53	429	434	434	2633	M. Borghini
22	ICHNUSSA13	48UR20131015	Urania	15 - 29 OCT 2013	37	405	404	405	3540	A. Ribotti
23	OCEANCERTAIN15	48QL20150804	Minerva Uno	4 - 29 AUG 2015	71	531	531	531	3513	J. Chiggiato
24	ICHNUSSA17/INFRAOCE17	48QL20171023	Minerva Uno	23 OCT - 28 NOV 2017	31	251	254	254	3536	A. Ribotti, S. Sparnocchia, M. Borghini



**Table 2**

Common name	EXPOCODE	Date Start/End	Source	Nutrient PI	Chief scientist
<i>M51/2</i>	06MT20011018	18 OCT - 11 NOV 2001	GLODAPv2	B. Schneider	W. Roether
<i>TRANSMED_LEGII</i>	48UR20070528	28 MAY - 12 JUN 2007	CARIMED	S. Cozzi, V. Ibello	M. Azzaro
<i>M84/3</i>	06MT20110405	5 - 28 APR 2011	GLODAPv2	G. Civitarese	T. Tanhua
<i>HOTMIX</i>	29AH20140426	26 APR - 31 MAY 2014	CARIMED	XA Álvarez-Salgado	J. Aristegui
<i>TALPro-2016</i>	29AJ20160818	18 - 28 AUG 2016	MedSHIP programme	L. Coppola	L. Jullion, K. Schroeder

**Table 3**

WOCE flag value	Interpretation in original dataset
2	Acceptable
3	Questionable/not used
9	Sample not measured/no data

**Table 4**

Cruise ID	EXPOCODE	std NO <sub>3</sub>	std PO <sub>4</sub>	std SiO <sub>2</sub>	# samples
1	48UR20040526	1.25	0.062	1.64	21
2	48UR20041006	0.59	0.029	0.81	21
3	48UR20050412	1.15	0.050	1.41	233
4	48UR20050529	1.13	0.057	1.08	205
5*	48UR20051116	1.35	0.078	0.98	16
6	48UR20060608	1.16	0.054	1.47	221
7*	06A420060720	-	-	-	-
8*	48UR20060928	0.71	0.036	0.76	179
9*	48UR20071005	0.89	0.040	0.86	302
10	48UR20080318	0.51	0.026	0.34	66
11	48UR20080905	-	-	-	-
12*	48UR20081103	1.11	0.077	0.10	110
13	48UR20090508	1.41	0.051	1.42	88
14	48UR20100430	1.06	0.036	1.03	159
15	48UR20100731	1.34	0.053	0.14	149
16	48UR20101123	1.02	0.045	1.02	14
17	48UR20110421	0.62	0.029	0.52	56
18	48UR20111109	0.68	0.025	0.70	77
19	48MG20111210	-	-	-	-
20	48UR20120111	0.97	0.051	0.26	152
21	48UR20121108	-	-	-	-
22	48UR20131015	1.03	0.043	0.79	98
23	48QL20150804	0.84	0.038	0.85	94
24	48QL20171023	0.68	0.055	1.24	55

(-) cruise not included in the 2<sup>nd</sup>QC

(\*) storage time >1 year



**Table 5**

Cruise ID	EXPOCODE	NO <sub>3</sub> (x)	PO <sub>4</sub> (x)	SiO <sub>2</sub> (x)
1	48UR20040526	1.14	1.23	1.21
2	48UR20041006	0.98	0.9	1.06
3	48UR20050412	1.08	0.93	1.15
4	48UR20050529	1.04	0.85	1.183
5	48UR20051116	1.19	1.34	1.232
6	48UR20060608	1.05	0.86	1.261
7	06A420060720*	-	-	-
8	48UR20060928	1.03	1.14	1.1
9	48UR20071005	0.97	1.14	1.115
10	48UR20080318	0.94	1.09	1.02
11	48UR20080905*	-	-	-
12	48UR20081103	1.08	1.38	1.12
13	48UR20090508	1.05	1.33	1.15
14	48UR20100430	NA	1.34	1.123
15	48UR20100731	1.13	1.25	1.262
16	48UR20101123	1.15	1.29	1.28
17	48UR20110421	NA	1.25	1.12
18	48UR20111109	NA	1.14	1.09
19	48MG20111210*	-	-	-
20	48UR20120111	NA	1.17	1.08
21	48UR20121108*	-	-	-
22	48UR20131015	NA	1.17	1.11
23	48QL20150804	1.02	1.02	1.08
24	48QL20171023	1.34	0.98	1.06

(\*) cruise not included in the 2<sup>nd</sup>QC but not removed from the final dataset



**Table 6**

Cruise ID	EXPOCODE	NO <sub>3</sub> [%]			PO <sub>4</sub> [%]			SiO <sub>2</sub> [%]		
		<i>n</i>	<i>unadjusted</i>	<i>adjusted</i>	<i>n</i>	<i>unadjusted</i>	<i>adjusted</i>	<i>n</i>	<i>unadjusted</i>	<i>adjusted</i>
1	48UR20040526	2	0.86	0.98	2	0.77	0.95	1	0.79	0.96
2	48UR20041006	2	1.02	1.00	2	1.10	0.99	1	0.94	0.99
3	48UR20050412	5	0.92	0.99	5	1.07	1.00	4	0.85	0.98
4	48UR20050529	5	0.96	1.00	5	1.15	0.98	4	0.82	0.99
5	48UR20051116	2	0.81	0.96	1	0.66	0.89	1	0.77	0.95
6	48UR20060608	5	0.95	1.00	5	1.14	0.99	4	0.74	0.93
7	06A420060720	0	-	-	0	-	-	0	-	-
8	48UR20060928	4	0.97	1.00	4	0.86	0.98	3	0.90	0.99
9	48UR20071005	5	1.03	1.00	5	0.86	0.98	4	0.88	0.99
10	48UR20080318	3	1.06	1.00	3	0.91	0.99	2	0.98	1.00
11	48UR20080905	0	-	-	0	-	-	0	-	-
12	48UR20081103	5	0.92	0.99	5	0.62	0.85	4	0.88	0.99
13	48UR20090508	3	0.95	1.00	3	0.67	0.90	2	0.85	0.98
14	48UR20100430	4	1.01	NA	4	0.66	0.88	3	0.88	0.99
15	48UR20100731	5	0.87	0.99	5	0.75	0.93	4	0.74	0.93
16	48UR20101123	1	0.85	0.98	1	0.71	0.91	1	0.72	0.92
17	48UR20110421	2	1.01	NA	2	0.75	0.94	1	0.88	0.99
18	48UR20111109	4	0.99	NA	4	0.86	0.98	3	0.91	0.99
19	48MG20111210	0	-	-	0	-	-	0	-	-
20	48UR20120111	4	1.01	NA	4	0.83	0.98	3	0.92	0.99
21	48UR20121108	0	-	-	0	-	-	0	-	-
22	48UR20131015	4	1.00	NA	4	0.83	0.97	3	0.89	0.99
23	48QL20150804	5	0.98	1.00	5	0.98	1.00	4	0.92	1.00
24	48QL20171023	3	0.66	0.88	3	1.02	1.00	2	0.94	0.99

\*red: data lower than reference